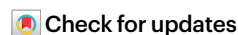


# Spatiotemporal co-optimization of agricultural management practices towards climate-smart crop production

Received: 24 February 2023

Accepted: 7 November 2023

Published online: 2 January 2024



Liujun Xiao<sup>1,2</sup>, Guocheng Wang<sup>3</sup>, Enli Wang<sup>4</sup>, Shengli Liu<sup>5</sup>, Jinfeng Chang<sup>1</sup>, Ping Zhang<sup>1</sup>, Hangxin Zhou<sup>1</sup>, Yuchen Wei<sup>1</sup>, Haoyu Zhang<sup>1</sup>, Yan Zhu<sup>2</sup>, Zhou Shi<sup>1</sup> & Zhongkui Luo<sup>1</sup>✉

Co-optimization of multiple management practices may facilitate climate-smart agriculture, but is challenged by complex climate–crop–soil management interconnections across space and over time. Here we develop a hybrid approach combining agricultural system modelling, machine learning and life cycle assessment to spatiotemporally co-optimize fertilizer application, irrigation and residue management to achieve yield potential of wheat and maize and minimize greenhouse gas emissions in the North China Plain. We found that the optimal fertilizer application rate and irrigation for the historical period (1995–2014) are lower than local farmers' practices as well as trial-derived recommendations. With the optimized practices, the projected annual requirement of fertilizer, irrigation water and residue inputs across the North China Plain in the period 2051–2070 is reduced by 16% (14–21%) (mean with 95% confidence interval), 19% (7–32%) and 20% (16–26%), respectively, compared with the current supposed optimal management in the historical reference period, with substantial greenhouse gas emission reductions. We demonstrate the potential of spatiotemporal co-optimization of multiple management practices and present digital mapping of management practices as a benchmark for site-specific management across the region.

Optimizing agricultural management practices has the potential to support sustainable agricultural intensification<sup>1,2</sup>. For example, integrated soil–crop system management experiments in China had improved fertilizer management with enhanced yields of major crops and reduced greenhouse gas (GHG) emissions<sup>2,3</sup>. These field-based experiments provide in situ data and promote mechanistic understanding of crop–environment management interactions, but are limited to specific locations and management practices. For multiple management practices

(for example, fertilizer application, irrigation and crop residue management), considering their nonlinear interactions and connections with local soil and climate dynamics<sup>4,5</sup>, it is difficult to target the optimal management combination by conducting field experiments and to generalize field-scale observations from limited locations<sup>1</sup>.

Agricultural management practices interact with local climatic and edaphic conditions to determine crop production and the relevant GHG emissions<sup>1</sup>. Irrigation and fertilizer applications, the two most common

<sup>1</sup>College of Environmental and Resource Sciences, Zhejiang University, Hangzhou, China. <sup>2</sup>National Engineering and Technology Center for Information Agriculture, Engineering Research Center of Smart Agriculture, Ministry of Education, Key Laboratory for Crop System Analysis and Decision Making, Ministry of Agriculture, Jiangsu Key Laboratory for Information Agriculture, Jiangsu Collaborative Innovation Center for Modern Crop Production, Nanjing Agricultural University, Nanjing, China. <sup>3</sup>Faculty of Geographical Science, Beijing Normal University, Beijing, China. <sup>4</sup>CSIRO Agriculture and Food, Canberra, Australian Capital Territory, Australia. <sup>5</sup>School of Agricultural Sciences, Zhengzhou University, Zhengzhou, China. ✉e-mail: [luozk@zju.edu.cn](mailto:luozk@zju.edu.cn)

practices to ensure high yield, affect almost all soil biogeochemical processes including GHG emissions<sup>6</sup>. Field studies have found synergies and trade-offs between multiple targets (for example, yield versus GHG emissions) under different management practices<sup>2,7</sup>. High yields usually rely on extensive use of fertilizer and irrigation water that, if not properly managed, may lead to high GHG emissions<sup>8</sup>. For example, experimental results in the North China Plain (NCP) indicated that total nitrogen application rate in wheat–maize double cropping system can be reduced from 600 to 330–420 kg ha<sup>-1</sup> per year and irrigation can be reduced by 240–350 mm ha<sup>-1</sup> per year with much less GHG emission without scarifying yield, but large uncertainties in such management exist among sites due to the variation of climate and soil conditions<sup>7</sup>.

Crop residue retention is another management focus for enhancing soil fertility and soil organic carbon (SOC) accumulation and thereby mitigating climate change<sup>9</sup>. However, SOC accumulation under more crop residue retention may require additional nutrient inputs to keep soil stoichiometric balance<sup>10</sup>. Excessive crop residue retention may break the stoichiometric balance, stimulate emissions of nitrogenous gases such as N<sub>2</sub>O<sup>11</sup> and thereby offset SOC accumulation and even reduce crop yield<sup>12</sup>. A synthesis of 176 long-term experiments showed that continuous crop residue retention on average is only effective for SOC accrual at the first 12 years<sup>13</sup>. Furthermore, future climate change affects crop growth, soil water and nutrient dynamics involving complex interactions between them. The management combinations of irrigation, fertilization and crop residues in theory should be also adapted to such climate change-induced crop growth-management feedbacks that, however, have been rarely assessed simultaneously<sup>10</sup>, particularly across large geographic regions and under long-term climate change conditions<sup>14</sup>.

In this article, we develop a hybrid approach combining biophysical agricultural system modelling, machine learning, life cycle assessment and multi-objective optimization techniques to derive optimal management combinations across space and over time (Fig. 1 and Methods). We first verify a widely used agricultural system model, the Agricultural Production System sIMulator (APSIM, Supplementary Fig. 1)<sup>15</sup>, to simulate crop productivity and environmental impacts under various climatic, soil and management conditions (across the NCP in this study—the ‘food bowl’ of China and a key area of global wheat and maize production, Supplementary Fig. 2). Then, machine learning emulators are trained to reproduce APSIM outputs (that is, wheat and maize yield, SOC changes and GHG emissions in this study) to facilitate high-resolution optimization and prediction across the region, which is otherwise difficult using the APSIM model alone. The best emulator is selected and combined with an evolution-based multi-objective optimizer to derive optimal management practice combinations (nitrogen (N) application, irrigation and residue management; Methods) to achieve at least 90% of maximum yield (which is defined as the yield without water and nutrient limitations) with minimum net GHG emissions (which take into account SOC changes and direct and indirect GHG emissions; Methods). In addition, we compare changes in the derived best management practices under both historical and future climate conditions to assess the effects of future climate change on the spatiotemporal dynamics of management, crop yield, SOC and net GHG emissions and to identify controlling factors over the potential spatiotemporal variability of optimized management practices.

## Results

### Model performance and simulation framework

The APSIM model explained 85%, 72%, 85% and 75% of the variances of the four variables (that is, wheat and maize yield, SOC dynamics and soil N<sub>2</sub>O emissions) observed in field experiments across the region, respectively (Supplementary Fig. 3). Using the verified APSIM model, we simulated a winter wheat–summer maize double cropping rotation system—the dominant cropping system in the study region—at

randomly selected locations under management scenarios with combinations of different levels of N input, irrigation water and residue retention (6,000 site-management simulations in total, Fig. 1). The simulations were conducted at a daily time step from 1981 to 2070. Daily future climate data were obtained by running general circulation models (GCMs) forced by historical daily climate records under two shared socio-economic pathways (SSPs; SSP2-4.5, the intermediate pathway of future GHG emissions, and SSP5-8.5, the most extreme pathway of future GHG emissions) and downscaled to the spatial resolution of 0.0083° (Supplementary Fig. 4 and Methods). Then, machine learning models (MLs) were trained against the simulation results to reproduce APSIM projections of crop yield, SOC dynamics and N<sub>2</sub>O emissions (Fig. 1 and Supplementary Fig. 5). The best ML—eXtreme Gradient Boosting (XGBoost)—was selected as the emulator of APSIM, which explains more than 96% of the variance of APSIM outputs (Supplementary Fig. 5) and captures main controls over the outputs (Supplementary Figs. 6–8).

Management practices were optimized to meet the target using a multi-objective optimizer during three periods (Methods), that is, 1995–2014 (historical reference period), 2021–2040 (near future) and 2051–2070 (distant future). Specifically, we conduct a multi-objective optimization including (1) at least 90% of maximum yield potential of both wheat and maize (which acknowledges that the 100% yield potential would actually never be achieved due to other constraints such as pest and disease and substantial diminishment of economic return above this figure<sup>16</sup>), (2) maximum SOC, (3) minimum net GHG emissions, (4) minimum N input, (5) minimum irrigation water and (6) minimum residue retention. The optimized management practices were compared to local farmers’ actual practice and to field trial-based recommendations (Methods).

### Crop yields and their responses to climate change

In the historical reference period 1995–2014, the optimized wheat yield is 7.2<sub>6.5</sub><sup>8</sup> Mg ha<sup>-1</sup> (mean with range across the region) across the NCP (Figs. 2a and 3a). Projected maize yield (8.1<sub>6.8</sub><sup>9.7</sup> Mg ha<sup>-1</sup>) is generally higher than wheat yield but with larger spatial variability (Fig. 2a versus 2b and Fig. 3b). The highest maize yield is projected in northeast NCP (Fig. 2b). Optimized wheat yield is higher than recorded wheat yield by local farmers as well as higher than the achieved yield by field experiments across the study region (Fig. 3a). For maize yield, it is generally close to both local farmers’ records and the achieved yield by field experiments (Fig. 3b).

Yield potential is defined as the yield of a cultivar when grown in environments without nutrients and water limitations. Under future climate change, maize yield potential is continuously decreased by up to 11.2–19.3% in the distant future compared with that during the historical reference period, while wheat yield potential remains relatively stable regardless of emission scenarios and climate projection models (Supplementary Figs. 9 and 10). Similar pattern of maize and wheat yield was projected under the optimal management (Figs. 2a,b and 3a,b). For maize, specifically, average yield across the region is reduced to 7.3 (that is, –10%) and 6.9 Mg ha<sup>-1</sup> (–15%) in the near (that is, 2021–2040) and distant future (that is, 2051–2070) under SSP2-4.5, respectively, compared with historical yield. A little more yield losses of maize are projected under SSP5-8.5 (Fig. 3b).

### SOC dynamics and net GHG emissions

In the historical reference period, NCP soils are carbon sinks at a rate of 0.48<sub>0.30</sub><sup>0.62</sup> Mg ha<sup>-1</sup> per year (Figs. 2c and 3c), which is comparable to field observations during a similar period (Fig. 3c) and other estimations in the same region<sup>17</sup>. However, the average SOC sequestration rate will slow down to about 0.2 Mg ha<sup>-1</sup> per year in the period 2021–2040 (Fig. 2c), confirming decline SOC accumulation after a relatively long-term crop residue return<sup>13</sup>. In the distant future (2051–2070), most NCP soils are projected to be close to carbon neutral, that is, reaching their carbon sequestration potential (Figs. 2c and 3c).

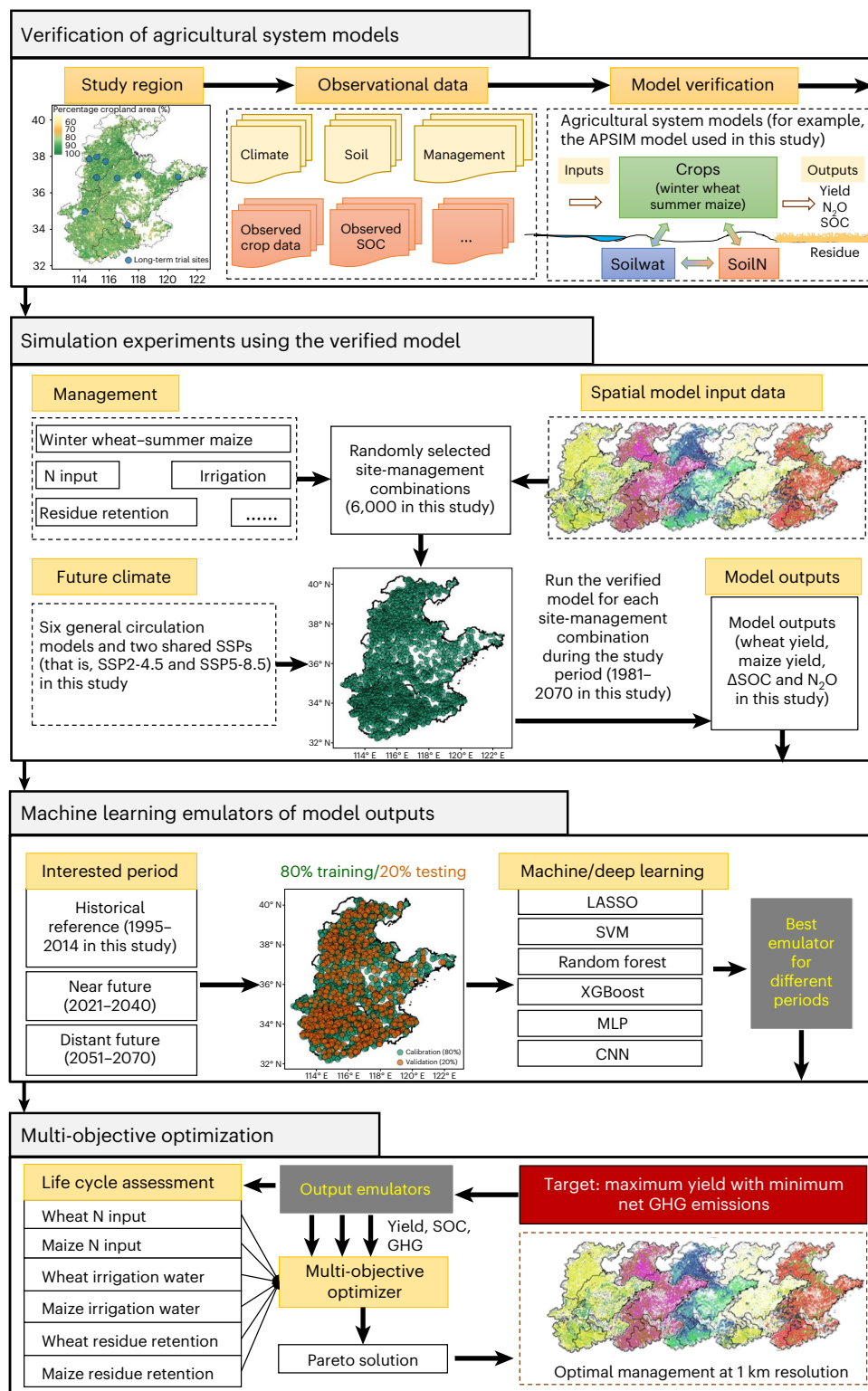


**Fig. 1 | A simulation framework enables spatiotemporal optimization of multiple management practices.** The framework combines verification of biophysical models, machine learning, life cycle assessment and multi-objective optimization to derive the best management combination across space and over time under targets of interests.

In the historical reference period, GHG emissions (which include direct N<sub>2</sub>O emissions caused by N fertilizer production and application, electricity usage for irrigation and residue retention and indirect N<sub>2</sub>O emissions from N volatilization and leaching, but do not include SOC changes that are considered separately; Methods) are

estimated to be  $8.0_{6.0}^{10}$  Mg CO<sub>2</sub>-eq ha<sup>-1</sup> per year across the region (Supplementary Fig. 11). The majority of GHG emissions (76%) are attribute to agricultural inputs (that is, fertilizer production and electricity for irrigation application), while the contribution of indirect N<sub>2</sub>O emissions and residue chopping is relatively small



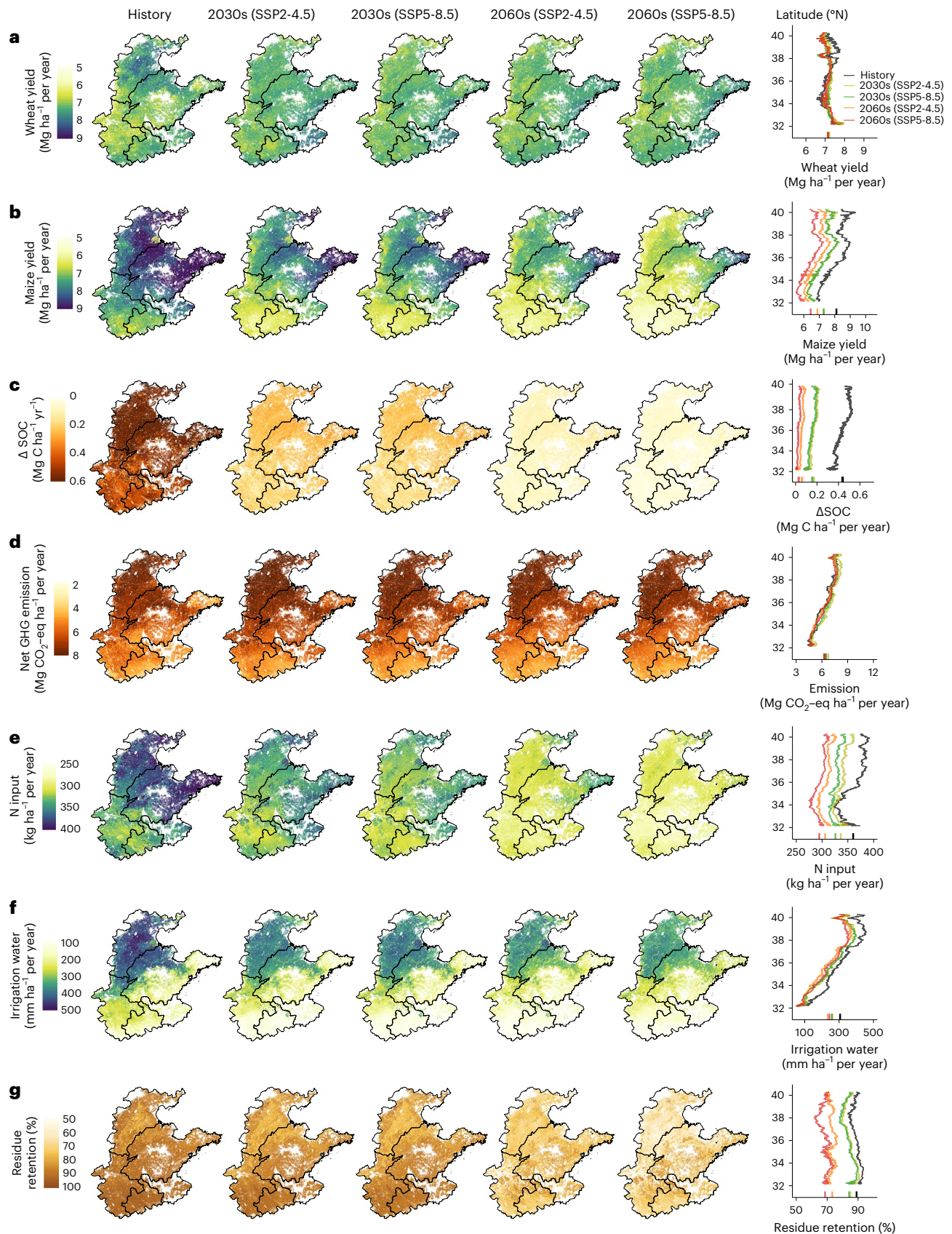


**Fig. 2 | Spatial pattern of yield, SOC changes ( $\Delta \text{SOC}$ ), net GHG emissions and optimized management practices under the target of maximizing yield and minimizing GHG emissions. a–d.** Panels from top to bottom show the projected annual average yield of wheat (a) and maize (b),  $\Delta \text{SOC}$  (c), net GHG emissions (d), N input (e), irrigation amount (f) and average residue retention fraction

(g), respectively, during the historical (1995–2014) and future periods (2030s: 2021–2040 and 2060s: 2051–2070) under two shared SSPs (SSP2-4.5 and SSP5-8.5). The value of each grid cell in the future periods shows the ensemble mean of all climate models. The rightmost panels show the relevant latitudinal pattern.



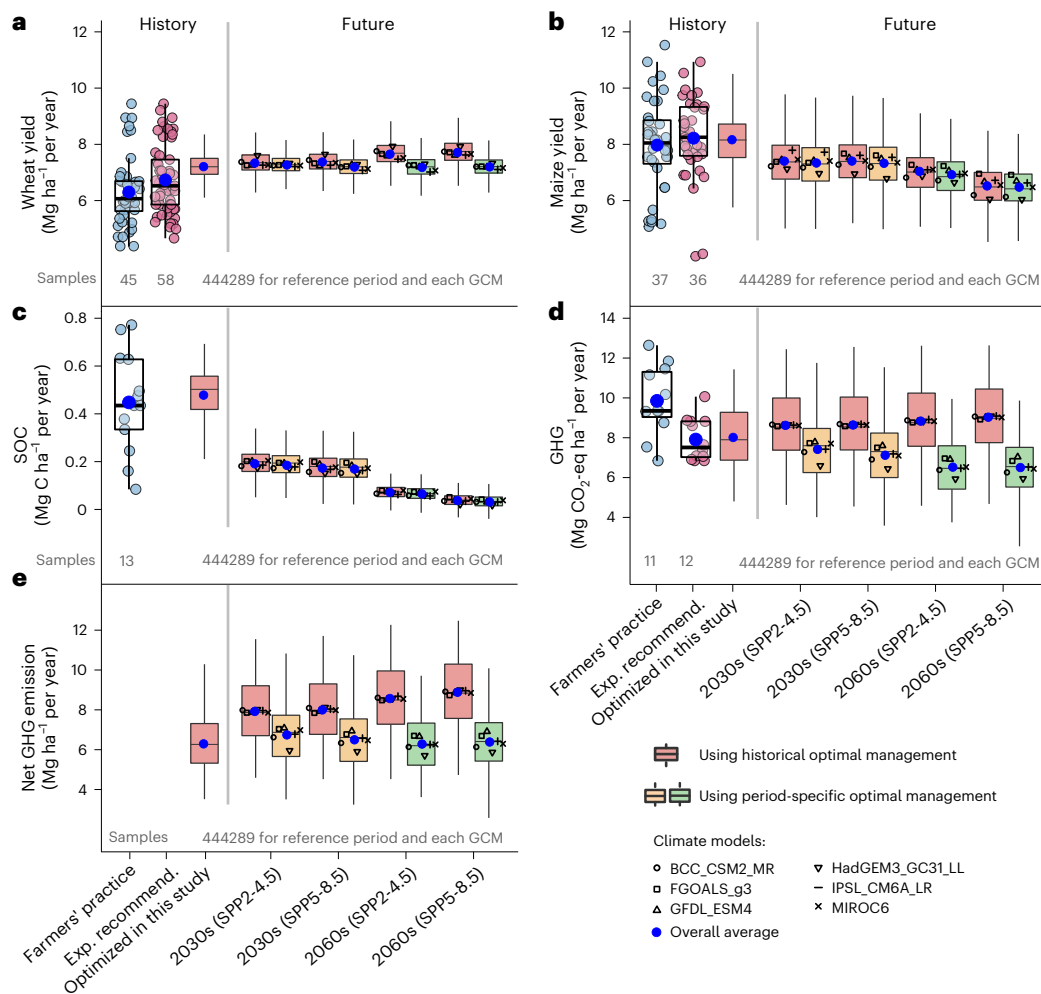


**Fig. 3 | Distributions of simulated yield,  $\Delta$ SOC and GHG emissions under the target of maximizing yield and minimizing GHG emissions across the study region (that is, the NCP). a–e.** Historical and projected annual yield of wheat (a) and maize (b),  $\Delta$ SOC (c), GHG emissions (d) and net GHG emissions (e). Historical projections (1995–2014) were compared with local farmers’ practices and field experiment-based recommendations (Exp. Recommend.; if the data are available). Future projections include two periods, 2030s (2021–2040) and

2060s (2051–2070) with climate projected by six climate models under SSP2-4.5 and SSP5-8.5, and are based on period-specific optimal management practices. Future projections using historical optimal management practices are also shown (light-pink boxplots). Boxplots show the median and interquartile range, with whiskers extending to the most extreme data point within  $1.5 \times (75\% - 25\%)$  data range. Solid blue circles show the average of projections for all climate models; other symbols show the projected average under each climate model.

(Supplementary Fig. 11). This estimation of GHG emissions is much lower than estimates based on local farmers’ practices, but comparable to estimates of field experiments (Fig. 3d). In the future, GHG emissions will decrease regardless of emission scenarios (Fig. 3d) due to decreased yield potential and consequently reduced requirement of fertilizers and irrigation water (see results below). SOC sequestration only plays a minor role in mitigating such GHG emissions in the future (Supplementary Fig. 11). As such, net GHG emissions (GHG emission – SOC change) across the region are close to total GHG emissions and are projected to be  $6.3^{8.0}_{4.4}$  Mg CO<sub>2</sub>-eq ha<sup>-1</sup> per year (Figs. 2c and 3e). In the future, due to synchronously decreased SOC sequestration rate with time (Fig. 3c), net GHG emissions are relatively stable during the whole simulation period (Fig. 3e), albeit GHG emissions are also reduced (Fig. 3d).

### Spatiotemporal pattern of optimal management practices

Across the region in the reference period, much more N is required at higher latitudes (Fig. 2e). The optimized N application rate for wheat and maize is  $190^{239}_{138}$  and  $168^{199}_{131}$  kg ha<sup>-1</sup>, respectively. These estimates are much lower than local farmers’ use of  $246^{302}_{179}$  and  $234^{253}_{132}$  kg ha<sup>-1</sup> during the similar period, respectively (Fig. 4a,b). Compared with the

recommended N application rate by field experiments conducted in the NCP (Methods), we predict a similar rate for wheat but much lower rate for maize (Fig. 4a,b). Under future climate change, less N, particularly for maize, is required (Fig. 4a,b) due to the negative effect of climate change on yield potential (Supplementary Figs. 9 and 10). In addition, the apparent latitudinal gradient of N requirement in the reference period narrows in general under future climate conditions (Fig. 2e).

Much more irrigation is required at higher latitudes across the region (Fig. 2f). In contrast to N input, this latitudinal gradient persists in the future (Fig. 2f versus 2e). Across the region, the irrigation amount is projected to be  $202^{325}_{80}$  mm for wheat and  $104^{162}_{27}$  mm for maize in the reference period, and is also lower than local farmers’ average practice of ~300 mm for wheat and ~151 mm for maize, but comparable to recommended amount by field experiments (Fig. 4c,d). In the future, the required irrigation water amount for wheat is substantially reduced by more than 20% depending on climate scenarios, while irrigation required for maize is slightly increased, particularly in the distant future under SSP5-8.5 (Fig. 4c,d). It should be highlighted that, if using the management practices optimized for the historical reference period in the future, it will result in much more GHG emissions in the two future

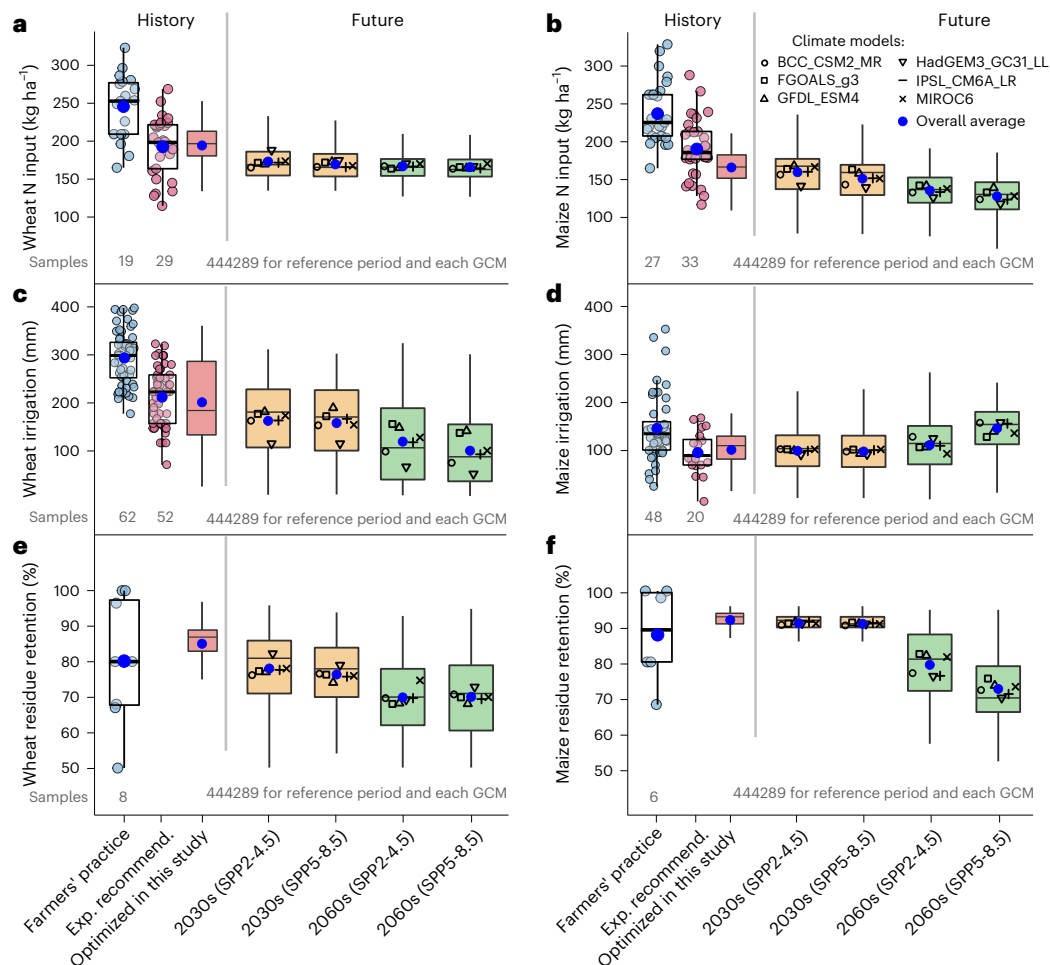


**Fig. 4 | Distributions of optimized management practices under the target of maximizing yield and minimizing GHG emissions across the study region (that is, the NCP). a–f,** Historical and projected annual wheat N input (a) and maize N input (b), wheat irrigation amount (c), maize irrigation amount (d), wheat residue retention (e) and maize residue retention (f). Historical projections (1995–2014) were compared with farmers’ practices and field experiment-based recommendations (Exp. Recommend.; if the data are

available). Future projections include two periods: 2030s (2021–2040) and 2060s (2051–2070) with climate projected by six climate models under SSP2-4.5 and SSP5-8.5. Boxplots show the median and interquartile range, with whiskers extending to the most extreme data point within  $1.5 \times (75\%–25\%)$  data range. Solid blue circles show the average of projections for all climate models; other symbols show the projected average under each climate model.

periods (+8% and +13% on average, respectively, Fig. 3c,d), albeit a small yield benefit for wheat (Fig. 3a).

It is intriguing to note that the optimal residue retention fraction is not 100% (that is, retaining all residues, Fig. 2g). This may be because residue retention stimulates SOC sequestration, but, on the other hand, it increases  $N_2O$  emissions (Supplementary Figs. 7 and 8). Thus, residue management should consider the trade-offs between SOC accrual and  $N_2O$  emissions. Averaging across the region, the optimized residue retention fraction is 85% for wheat and 93% for maize, which are slightly higher than local farmers’ practice (which is 68% for wheat and 85% for maize, Fig. 4e,f). The optimized fraction of maize residue retention is generally higher than that of wheat in the whole simulation period regardless of climate scenarios. In the near future, optimal wheat residue retention fraction is decreased by 7.2% under SSP2-4.5 and 9.2% under SSP5-8.5, while maize residue retention keeps relatively stable. In the distant future, however, the retained fraction of wheat and maize residues consistently shows a decreasing trend under both SSP2-4.5 and SSP5-8.5 (Fig. 4e,f).

### Drivers of the optimal management

Linear mixed-effects regression is conducted to test the effects of environmental factors on each optimized management practice treating

simulation period (that is, historical reference period, near future and distant future) as a random effect (Methods and Fig. 5). Averaging across the simulation periods, the effects of mean annual temperature (MAT) and mean annual precipitation (MAP) on wheat-season irrigation are significantly negative and the strongest (Fig. 5a). The magnitude and direction of the effects of the assessed variables vary among the management practices. Some variables showed significant effects on particular management practices, but insignificant on other practices (Fig. 5a). Among the simulation periods, the effects of the assessed variables on all management practices are significantly different (Fig. 5b,d). Overall, these results indicate that the effects of different variables on management practices are time dependent (Fig. 5). In addition, management practices are closely correlated to each other regardless of averaging across the three periods or during each simulation period (Fig. 5). It is intriguing to note that the strongest association occurs between maize-season N input and wheat-season irrigation for wheat–maize rotation, particularly in the two future periods (Fig. 5a,c,d).

Due to the complex associations of management practices with environmental variables (Fig. 5), we conduct a variance partitioning analysis (VPA) to explore the overall influence of the assessed environmental variables (with the consideration of their interactions)

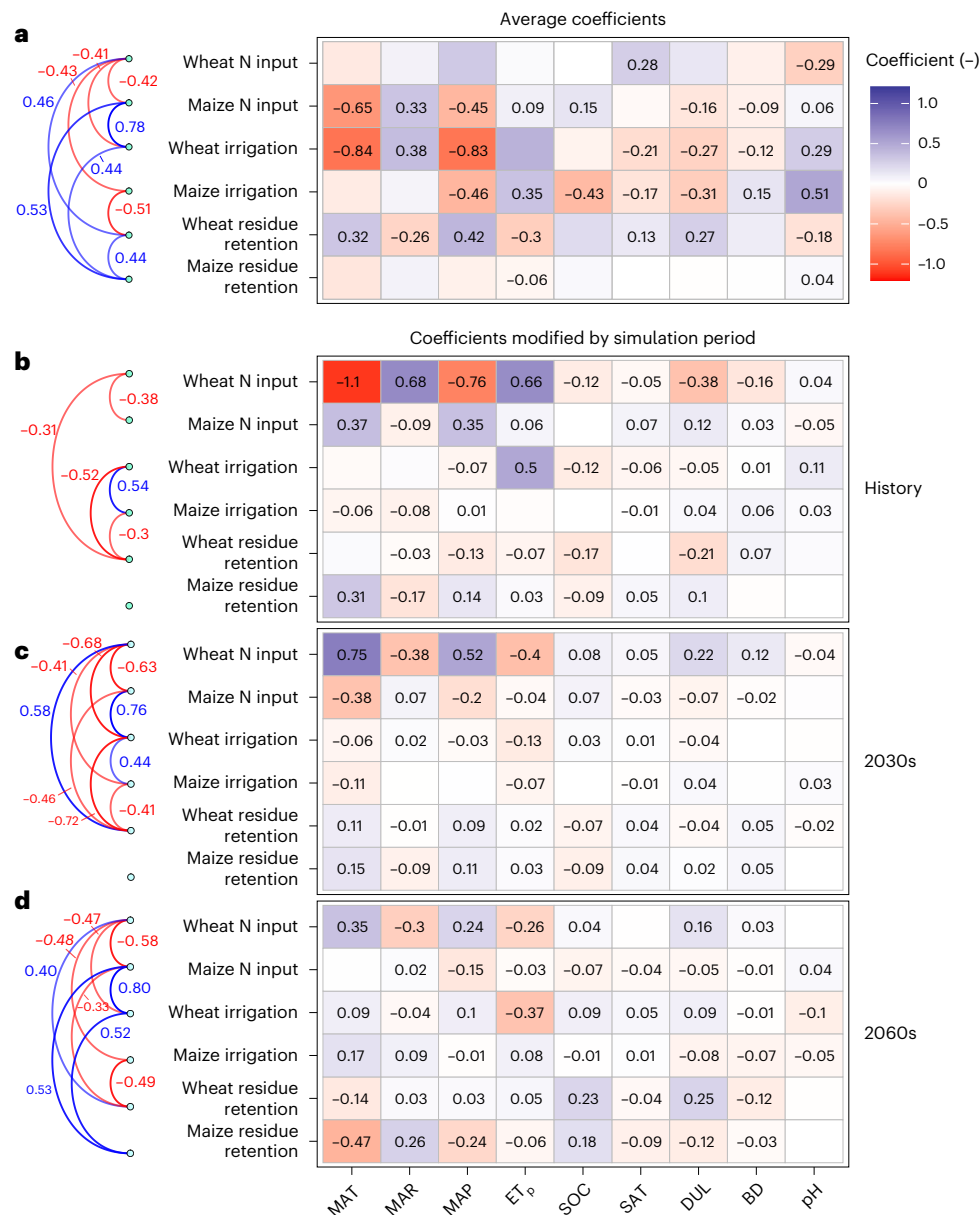


**Fig. 5 | Coefficients of the predictors of a linear mixed-effects regression for optimized management practices.** Simulation period (that is, historical reference period, 2030s: 2021–2040 and 2060s: 2051–2070) is treated as a random effect. **a**, average coefficients (that is, fixed effect) across the three simulation periods. **b–d**, coefficients modified by three simulation periods. Curves connecting the management variables on the left indicate that the

correlation between the two managements is significant with the numbers showing correlation coefficients (Pearson's  $r$ ). Two-sided tests should be used. Only were significant (that is,  $P < 0.05$ ) coefficients shown in italic bold font. ET<sub>p</sub> is the potential evapotranspiration; SOC, SAT, DUL, BD and pH are the SOC content, water content at the saturation point, field capacity of water content, bulk density and pH, respectively.

in influencing optimal management practice combinations across the region (Methods). The VPA explains 65% of the variance of optimal management combinations (Supplementary Fig. 12). The interaction between water-related factors (that is, MAP and potential evapotranspiration and temperature-related factors (that is, MAT and mean annual radiation (MAR)) is the most important individual factor, alone explaining 17.7% of the total variance. Water-related factors, the interaction between water-related factors and soil properties and soil properties explain 11.9%, 9.7% and 8.6% of the variance, respectively. Other variables or interactions explain less than 3% of the variance (Supplementary Fig. 12). Overall, water-related factors are the predominant factor. Their individual effects and sharing in their interactions with other variables together explain 29.3% of the variance (that is, accounting for 45% of the total explained variance),

followed by soil properties (14.3%) and temperature-related factors (13.7%, Supplementary Fig. 12).

## Discussion

### Crop type-dependent response of yield to climate change

Our results suggest that maize is more vulnerable to future climate change than wheat in the NCP, which has been also found in other regions<sup>18</sup>. For wheat, the reason may be that, although winter warming poses a negative effect on wheat growth<sup>19</sup>, this can be offset by fertilization effect of elevated CO<sub>2</sub><sup>18</sup>. It is also general that elevated CO<sub>2</sub> has a weaker fertilization effect on the growth of C4 plants like maize than C3 plants like wheat<sup>20</sup>. However, the positive fertilization effect of elevated CO<sub>2</sub> on plant growth will be saturated if CO<sub>2</sub> concentration increases to certain level in the future<sup>20</sup>. Moreover, summer maize is



very sensitive to summer high temperature that is closely associated with heatwaves and drought<sup>21</sup> and common in summer under global warming (Supplementary Fig. 4). We propose that careful selection of cropping systems including crop type and their rotation may have the potential to alleviate the negative effect of climate change<sup>22</sup>.

### Optimal management practices over time and space

Optimizing management practices with time saves water and fertilizers and thus reduces relevant GHG emissions under future climate change. We projected much higher productivity per unit N and water use than local farmers' practice and field experiment-based recommendations (Supplementary Fig. 13). This implies the importance of fertilization time for improving nutrient use efficiency<sup>2,7,23</sup>. As irrigation and fertilization are the major contributors to total GHG emissions, reduced fertilizer and water inputs could substantially reduce GHG emissions, offsetting the decline of SOC sequestration rate (that is, SOC saturation)<sup>24</sup>.

Our results confirm that NCP soils were a carbon sink in history<sup>17</sup>. However, this value cannot be maintained even in the near future (2021–2040) as soils gradually reach their SOC sequestration potential. The optimized amount of crop residue retention was projected to reduce in the future because more residue inputs contribute less to SOC sequestration due to SOC saturation<sup>12,24</sup>, but stimulate soil N<sub>2</sub>O emissions<sup>23</sup> and induce other constraints such as limiting seed germination. The optimum retention fraction depends on the total amount and type of residues, soil properties and climate conditions<sup>9</sup>. Indeed, our simulations predict large spatial variability of the optimal retention fraction across the study region (Fig. 2g). Although crop residue retention may have positive effects on overall soil health<sup>9</sup>, our modelling results highlight that residue retention would be a double-edged sword.

Optimal management practices are strongly associated with both climatic and edaphic conditions. Despite water-related factors (for example, MAP and evapotranspiration) and temperature-related factors (MAT and MAR) being the most important factors influencing optimal management combinations, soil conditions may play a vital role in regulating water and nutrient availability for plant growth and may therefore be the relevant management practices. In the NCP, as an alluvial plain that has experienced thousand years of cultivation, soil conditions are relatively homogeneous but still show similar magnitude of importance as climate. Indeed, this importance is under-recognized<sup>25,26</sup> and needs to be further elucidated particularly in terms of buffering environmental influences.

### Limitations and recommendations

Some limitations remain in our simulations. First, the quality of spatial data that are required for process-based modelling is usually difficult to control. Especially, we emphasize that accurate three-dimensional soil data such as vertical distribution of soil nutrients and water holding capacity along soil profile will be invaluable for understanding soil–plant management interactions. Second, although process-based models like APSIM depict key processes regulating agricultural system dynamics in response to management and environment, they have their own deficiencies due to imperfect understanding of relevant processes. For example, few models, if not none, have verified their ability to simulate the effects of extreme climate (such as high-temperature impact on pollination and seed set and so on) and the role of soil in buffering environmental influences<sup>27</sup>. Third, we used the same wheat and maize cultivars during the whole simulation period and thus did not consider climate adaptation offered by crop genetic potential<sup>28</sup>. Gene-driven breeding may enable new varieties with a higher yield potential and increased water and nutrient use efficiency<sup>29</sup>, thereby reducing water and nutrient requirements and finally reducing GHG emissions. By adopting genetically modified cultivars with higher yield potential would change management practices, which need to be explicitly explored in future work.

Our results demonstrate the great potential of co-optimizing multiple management practices for securing crop production with less resource input and environmental costs. To promote the implementation of such optimized management practices, we suggest the three aspects of actions in terms of scientific research, farmer engagement and government policy. First, national and international multidisciplinary research network is needed to comprehend the complex processes and interactions between climate, soil, crops and management, to holistically and fully realize the potential of sustainable agriculture and to develop effective site-specific solutions<sup>30</sup>. Agricultural system models (for example, APSIM) integrating climate–plant–soil management interactions can play an important role, facilitating mechanistic understanding and the derivation of management practices and future response at the spatiotemporal resolution meaningful for farmers' practice<sup>31</sup>. Second, it needs to effectively engage and persuade farmers, particularly smallholders like in the NCP and China, who usually receive less education and restricted access to innovative solutions and practices and are more vulnerable to economic variability. Involving local farmers and communities in the identification and confirmation of the optimal practices will build up farmers' successful experience and thus confidence and willingness to adopt the practices. The Science and Technology Backyard in China is a successful example of unlocking the potential of smallholder farmers<sup>32</sup>. Finally, but not less important, by offering financial and market incentives, subsidies, grants and supportive policies, government can act as a bridge to connect and support scientific research and farmers' implementation. For example, China's 14th 5-year plan promotes the investment of national field experiment network and implementation of smart agriculture practices<sup>33</sup>, which will promote the study of sustainable agriculture and the implementation of the best practices.

### Conclusion

Co-optimization of multiple management practices is challenging via field experimental approaches due to complex climate–soil–crop management interactions that highly vary across space and over time. We propose a modelling framework to explore such spatiotemporal variabilities and derive optimal management practice combinations for climate-smart agricultural intensification. Applying the framework in the NCP, the simulation results suggest great potential of saving fertilizer and water resources and reducing GHG emissions without sacrificing much yield in the NCP under future climate conditions. Importantly, future management practices should be adjusted with climate change as yield potential would be damaged by future climate if not using cultivars adapted to climate change, and thus less resource input is required. Overall, co-optimization of multiple management practices can enhance our ability to secure environmentally friendly food production under climate change. Together with advancing crop breeding techniques, the expediting accumulation of three-dimensional soil data and the improving understanding and modelling of plant–soil interactions are paving the way for climate-smart agricultural production under smart management across space and over time.

### Methods

We develop a framework combining biophysical models, life cycle assessment, machine learning and multi-objective optimization techniques to co-optimize multiple management practices at spatiotemporal resolutions meaningful for land management (Fig. 1). The framework is applied to a typical region—the NCP—in China to identify optimal management practice combinations to achieve an integrated target of maximizing yield and SOC sequestration and minimizing GHG emissions.

### The study region

The NCP (Supplementary Fig. 2, the boundary is consistent with ref. 31) is the largest agricultural production region in China, producing

~33% and ~60% of China's maize and wheat, respectively<sup>34</sup>. The dominant cropping system in the region is irrigated winter wheat–summer maize double cropping rotation with an average growing season from October to June for wheat and from June to September for maize<sup>35</sup>. The NCP is a region characterized by a summer monsoon climate. The MAT in the region ranges from 11 °C to 17 °C and MAP from 461 mm to 1,033 mm during the period 1995–2014. In NCP, to maintain high yield, a large amount of groundwater is exploited for irrigation with an annual average usage of 400–450 mm (70% used for wheat) in the past decades, resulting in groundwater depletion. The average N fertilizer usage of local farmers is ~246 kg N ha<sup>-1</sup> per year for wheat and ~234 kg N ha<sup>-1</sup> per year for maize (Fig. 4). However, the use efficiency is low with a value of less than 30%, causing a series of environmental problems relating to N pollutions and GHG emissions<sup>36</sup>. Excessive resource (for example, nitrogen and water) consumption and intensive cultivation result in soil degradation, challenging sustainable agricultural intensification in NCP<sup>8</sup>. Optimizing management practices to sustain crop production, maintain soil health and minimize associated environmental footprints in the NCP has become a priority of both the regional and national central government.

### Climate and soil datasets

Daily historical meteorological data at ~2,400 climate stations across China (including 318 stations in NCP), including maximum temperature, minimum temperature, precipitation, sunshine hours, relative humidity and wind speed, were obtained for the period 1981–2014 from the Chinese Meteorological Administration (<http://data.cma.cn>). Daily solar radiation required by the APSIM model (see the 'The APSIM model' section) was calculated by daily sunshine hours. We employed a statistical downscaling approach combining with the thin plate spline regression method and machine learning (using R package *machispln* for R v4.0.5)<sup>37</sup> to interpolate the observed meteorological data to the whole country at the resolution of ~1 km (0.0083°). Spatial climate data in the NCP, which is required for regional simulations, were extracted from the downscaled national mapping products.

Daily climate during the period from 2015 to 2070 was projected by six GCMs (including BCC\_CSM2\_MR, HadGEM3\_GC31\_LL, FGOALS-g3, IPSL\_CM6A\_LR, GFDL\_ESM4 and MIROC6; Supplementary Table 1) participating in the Coupled Model Inter-comparison Project phase 6 (CMIP6)<sup>38</sup>, under two shared SSPs. The shared SSPs are represented by SSP2 with RCP4.5 (here SSP2-4.5) and SSP5 with RCP8.5 (here SSP5-8.5). They were selected as the intermediate and the most extreme anthropogenic radiation forcing increases<sup>39</sup>, respectively. We used the historical climate data during the period 1981–2014 to bias-correct CMIP6 climate model outputs based on the ISIMIP3b method<sup>40</sup> and downscaled the projected future climate using the same approach for downscaling historical data. During the period 2015–2070, the results indicate that mean temperature and precipitation are increased by 1.7–2 °C and 15.6–15.8% in the wheat growing season (that is, from October to June), respectively, and by 1.7–2 °C and 17.2–18.2% in the maize growing season (that is, from June to September), respectively, depending on GCMs (Supplementary Table 1 and Supplementary Fig. 4). Future atmospheric CO<sub>2</sub> concentration used in CMIP6 for SSP2-4.5 and SSP5-8.5 (Supplementary Fig. 4) has also been obtained to model the fertilization effect of CO<sub>2</sub> on plant growth.

Soil data in the NCP were obtained from the China Soil Scientific Database<sup>41</sup> at the same resolution of climate data (that is, ~1 km), which was generated on the basis of more than 7,000 soil profile measurements in the late 1970s/early 1980s across China and is the most comprehensive soil data available. Major soil properties include SOC content, total nitrogen content, bulk density, clay fraction, pH, saturated water content and drained upper limit and lower limit of crop water extraction in different soil layers down to 2.5 m, which are required to drive the APSIM model.

### Observational data for model verification

We conducted a literature search to collect data about yield and relevant application of N fertilizers, irrigation amount and residue retention (Supplementary Table 2 and Supplementary Data). A total of 307 observations including 108 values of N fertilizer use from 33 studies, 182 values of irrigation water use from 38 studies and 17 values of residue retention fraction from 7 studies were obtained. The observational practices can be divided into two general types: local farmers' actual practice and field experiment-based recommendation of management practices. We calculated the N productivity and irrigation productivity (Supplementary Fig. 11) as the ratio of yield to corresponding N input and irrigation amount. All data have been grouped into two types (that is, local farmers' practice and field-based recommendation) and compared with model projections in the similar period at the regional level. In addition, we extracted data from 12 long-term agricultural trials from 11 studies on long-term SOC changes and 17 from 6 studies on N<sub>2</sub>O and GHG emission with current local farmers' conventional and recommended management practices for winter wheat–summer maize system during 1980–2017 in the region studied.

In addition, we collected data from nine long-term agricultural trials conducted in the NCP as a part of the National Long-term Fertilization Experimental Network in China<sup>42</sup>. Specifically, all trials focus on the winter wheat–summer maize rotation system under different management treatments. We extracted data of crop yield, SOC and N<sub>2</sub>O emissions to validate the performance of the APSIM model on predicting these variables (Supplementary Fig. 2). More detailed information on the nine long-term trials are described in Supplementary Table 3.

### The APSIM model

The APSIM<sup>45</sup> was used to simulate climate–plant–soil interactions and impact of management intervention on a daily time step using daily climate generated by the six climate models under two shared SSPs (that is, a total of 12 climate scenarios). The model simulates plant phenological development from sowing to maturity in response to temperature, vernalization (wheat) and photoperiod. Daily plant growth is simulated using plant development stage-dependent radiation use efficiency constrained by temperature, water and nitrogen availability. Soil organic matter is divided into four pools distinguished by decomposability, namely, fresh organic matter (FOM), microbial biomass, humus and an inert organic matter pool<sup>43</sup>. The decomposition of FOM, microbial biomass and humus is defined as a first-order decay process modified by temperature, moisture and nutrient availability and results in the release of CO<sub>2</sub> to the atmosphere and transfer of the remaining decomposed carbon to other pools<sup>44</sup>. The flows between different pools are calculated in terms of carbon. The corresponding N flows depend on the carbon flow into the receiving pool and its C:N ratio. The C:N ratios of various pools except FOM were assumed to be constant through time. APSIM simulates direct N<sub>2</sub>O emissions from both nitrification and denitrification processes<sup>45</sup>. The N<sub>2</sub>O emission from the nitrification process is estimated as a fraction of nitrified N, with the latter modelled by Michaelis–Menten kinetics treating soil ammonium as the substrate, and modified by soil pH, soil moisture and temperature. Denitrification-induced N<sub>2</sub>O emission is calculated by multiplying the denitrification rate by the ratio of N<sub>2</sub> to N<sub>2</sub>O emitted from denitrification adopted from the DayCent model<sup>45</sup>. In addition, APSIM allows flexible specification of management practices such as crop and rotation type, sowing and harvesting rules, fertilizer application, manure application, irrigation and residue management.

The ability of APSIM to simulate yield, soil carbon and nitrogen dynamics together with other processes in response to management practices have been comprehensively verified worldwide<sup>31,46</sup>. In the NCP, specifically, APSIM parameters have been widely calibrated and verified to simulate various aspects of wheat–maize cropping system (which is the target system of this study) at different sites in previous studies<sup>47</sup>. Cultivar parameters of wheat and maize and model

parameters relating to soil organic matter dynamics, nitrification and denitrification have been carefully validated in the NCP in our previous studies<sup>31,47</sup>. We further verified the ability of the APSIM model in simulating yield, SOC dynamics and N<sub>2</sub>O emissions using collected from nine long-term trials as described above (Supplementary Fig. 3).

### Hybrid simulations combining APSIM and machine learning

We simulated the common winter wheat–summer maize rotation system at ~1 km resolution across the NCP croplands (a total of  $\sim 4.4 \times 10^5$  grid cells) using a hybrid approach of combining the APSIM model and machine learning-based emulators of APSIM outputs (Fig. 1). First, the APSIM model was run for the period 1981–2070 under scenarios of N application, irrigation, crop residue management, climate change and their combinations. As our purpose is to identify the optimal management, we built fine-tuning scenarios. Specifically, the N application scenario ranges from 0 to 400 kg N ha<sup>-1</sup> per year for each crop season with an increment of 1 kg N ha<sup>-1</sup> per year. If the N application was less than 30 kg N ha<sup>-1</sup>, 100% of N was applied as a basal fertilizer application at the time of sowing for both crops; if it was greater than 30 kg N ha<sup>-1</sup>, 40% of the total N was applied as base fertilizer and any additional N was being applied at the stem elongation of wheat and leaf appearance stage of maize as a top dressing. For all scenarios, other nutrients (for example, phosphorous and potassium) are assumed to be efficient and do not limit crop growth. Irrigation scenario includes no irrigation; one (at sowing time), two (additional irrigation at floral initiation), three (additional irrigation at flowering) and four times (additional irrigation at the start of grain filling) of irrigation (irrigated to the field capacity in the top 50 cm soil); and auto-irrigation (that is, irrigating once soil water content drops to drained lower limit). Crop residue management ranges from 0% to 100% removal with an increment of 5% for both wheat and maize. Climate scenarios include the combinations of the six GCMs and the two SSPs. In total, there are  $\sim 1.0 \times 10^{14}$  management–climate scenario combinations, which is impossible to simulate using the APSIM model in a reasonable time for all grid cells. To solve this computational challenge, 6,000 grid scenarios were randomly drawn to run the APSIM model. That is, for each drawing, one grid and one management–climate scenario were randomly selected from the  $\sim 4.4 \times 10^5$  grids and  $\sim 1.0 \times 10^{14}$  management–climate scenarios, respectively. The 6,000 random samples are almost evenly distributed across the NCP and can well represent the population of scenario combinations including all scenario possibilities. APSIM-projected SOC in the whole soil profile (that is, 0–2 m), wheat and maize yield and soil N<sub>2</sub>O emissions were output. Average annual SOC change ( $\Delta$ SOC), crop yield and N<sub>2</sub>O emissions during the period 1995–2014 (as the historical reference period), 2030s: 2021–2040 (represents near future) and 2060s: 2051–2070 (represents distant future) were calculated.

Then, we trained six types of ML driven by three categories of predictors (that is, soil, climate and management; Supplementary Table 4) to emulate APSIM-projected  $\Delta$ SOC, average yield and N<sub>2</sub>O emission during the three periods. The six MLs are generalized linear model with lasso penalty (GLMNET), support vector machines, random forest, XGBoost, multilayer perceptron neural network and convolutional neural network. For climate variables, to reflect their temporal variability and effects on the development of crops, we first calculated the three-hourly temperature for each day using daily maximum and minimum temperatures<sup>27</sup>. Using the three-hourly temperature, two bins of growing degree days ( $GDD_{low}$ , thermal time between  $T_{base}$  (base temperature) and  $T_{opt}$  (optimum temperature);  $GDD_{high}$ , thermal time between  $T_{opt}$  and  $T_{max}$  (maximum temperature)), cold degree days (thermal time below  $T_{base}$ ) and heat degree days (thermal time above  $T_{max}$ ) were calculated and then accumulated throughout the growing season for wheat and maize, respectively.  $T_{base}$ ,  $T_{opt}$  and  $T_{max}$  are 0, 26 and 34 °C for wheat and 8, 30 and 42 °C for maize, respectively.

Eighty per cent of the 6,000 grid-scenario simulation outputs were randomly selected for training the six MLs and the remaining 20% for

validation. The root mean squared error and determination coefficient ( $R^2$ ) were used to evaluate model performance. XGBoost was consistently the best ML emulating APSIM-projected  $\Delta$ SOC, average yield and N<sub>2</sub>O emission and explained more than 95% of their variances (Supplementary Fig. 5 and Supplementary Table 5). As such, the XGBoost model was selected as the emulator of APSIM and used to optimize yield, SOC dynamics and soil N<sub>2</sub>O emission under various management practices in each 0.0083° grid cell across the region.

### Estimation of GHG emissions

Coupling with  $\Delta$ SOC and N<sub>2</sub>O emissions projected by the APSIM model, a life cycle assessment-based evaluation method<sup>48</sup> was used to estimate net GHG emissions in CO<sub>2</sub> equivalent (CO<sub>2</sub>-eq ha<sup>-1</sup> per year) of three components (Eqs. (1)–(4)): (1) GHG emissions of resource input caused by input supply chain (Input<sub>emission</sub>, for example, fertilizer production, transport and combustion of fossil fuels), (2) direct and indirect N<sub>2</sub>O emissions caused by the application of N fertilizer (N<sub>2</sub>O<sub>emission</sub>) and (3) SOC changes ( $\Delta$ SOC):

$$GHG_{emission} = Input_{emission} + N_2O_{emission}, \quad (1)$$

where

$$Input_{emission} = N_{input} \times EF_{Ninput} + Irr \times 9.2 \times EF_{irr} + SR \times (EF_{chopping} + EF_{incorporation}) \quad (2)$$

$$N_2O_{emission} = N_2O_{directemission} + N_2O_{indirectemission} \quad (3)$$

$$N_2O_{directemission} = N_2O_{APSIM} \times \frac{44}{28} \times GWP \quad (4)$$

$$N_2O_{indirectemission} = (N_{input} \times 0.1 \times EF_{Nvol, N_2O} + N_{input} \times 0.3 \times EF_{Nleach, N_2O}) \times \frac{44}{28} \times GWP \quad (5)$$

$$C_{emission} = -\Delta SOC \times \frac{44}{12} \quad (6)$$

$$Net\ GHG_{emission} = Total\ GHG_{emission} + C_{emission}, \quad (7)$$

where  $GHG_{emission}$  are the total GHG emissions and  $Input_{emission}$  is the GHG emissions from agricultural inputs, including N fertilizer production (cradle to gate), electricity for irrigation, straw chopping and incorporation. GWP is the 100-year global warming potential of N<sub>2</sub>O, which is 265 in the Intergovernmental Panel on Climate Change (IPCC)<sup>49</sup>.  $N_{input}$  (kg N ha<sup>-1</sup>),  $Irr$  (mm) and  $SR$  (%) are the N inputs from N fertilizers, irrigation amount and the fraction of crop residues retained, respectively.  $EF_{Ninput}$  is the GHG emission factor of N fertilizer production (Supplementary Table 6); 9.2 (kWh<sup>-1</sup> mm<sup>-1</sup>) is the electricity consumption per unit irrigation water application (mm);  $EF_{irr}$  is the GHG emission factor of electricity by irrigation;  $EF_{chopping}$  and  $EF_{incorporation}$  are GHG emissions for crop residue chopping and incorporation for maize.  $N_2O_{APSIM}$  is the annual cumulative amount of APSIM-projected N<sub>2</sub>O emission (kg CO<sub>2</sub>-eq ha<sup>-1</sup>) resulting from nitrification and denitrification;  $EF_{Nvol, N_2O}$  and  $EF_{Nleach, N_2O}$  are N<sub>2</sub>O emission factors induced by N volatilization and leaching, respectively; 0.1 and 0.3 are the fractions of volatilized and leached N, respectively, derived from IPCC 2006<sup>50</sup>. Emission factors used in these equations are derived from previous studies or values suggested by the IPCC (Supplementary Table 6).

### Co-optimization of multiple management practices

Using the XGBoost model, we first projected the maximum yield potential for each grid cell under each climate scenario using a differential



evolution algorithm<sup>51</sup>. Then, management practices (that is, minimum N input, irrigation amount and residue retention) under each climate scenario were optimized to achieve at least 90% of the maximum yield potential plus minimum net GHG emissions and maximum SOC sequestration.

We performed a multi-objective optimization algorithm (Non-dominated Sorting Genetic Algorithm II, NSGA-II) to search the global optimal management practices for the target. NSGA-II is a fast sorting and elite multi-objective genetic algorithm for searching the Pareto-optimal front (a set of solutions that define the best trade-offs between competing objectives)<sup>52</sup>. To build the objective function, the best machine learning emulators (that is, XGBoost) were wrapped to predict the variable of  $\Delta$ SOC, wheat and maize yield and  $N_2O$  emission. Management practices were treated as parameters of objective functions to be optimized. The parameters were firstly set a boundary with lower and upper values (that is,  $0 \text{ kg ha}^{-1} \text{ per year} \leq N_{\text{input}} \leq 400 \text{ kg ha}^{-1} \text{ per year}$ ,  $0 \text{ mm} \leq \text{irrigation water use} \leq 600 \text{ mm}$ ,  $0 \leq \text{residue retention fraction} \leq 100\%$ ) for both wheat and maize seasons. Pareto solution set was obtained through multiple iteration runs by comparing objective function values in NSGA-II (Supplementary Fig. 14). This Pareto solution set includes several preferable management practices (Supplementary Fig. 14); the management combination with maximum yield was selected as the final best one. By conducting the optimization for each grid, we obtained digital maps of management at the resolution of  $0.0083^\circ$  as well as the corresponding yield, GHG emissions and SOC sequestration values.

### Environmental controls on optimal management

We randomly sampled 50,000 points of optimized management combinations from their mapping products in the NCP at a resolution of  $\sim 1 \text{ km}$  and explored the influence of a set of environmental covariates including climate variables (MAT, MAP, MAR, potential evapotranspiration ( $ET_p$ ) and so on) and soil properties (that is, pH, SOC, bulk density, SAT and so on) on the optimized management practices. Correlation analysis was conducted to assess the pairwise associations among individual management practices. In addition, linear mixed-effects regression (using the 'lmer' function of the 'lmerTest' package in R) was performed to identify the effects of environmental covariates on optimal management by climate models as the random effect factor. At last, a VPA based on redundancy analysis (RDA)<sup>53</sup> was conducted to assess the controlling factors of the best management combination using R package UPSetVP. RDA models the effect of an explanatory matrix on a response matrix (that is, the optimized management practices in this study). Combining RDA with VPA, the approach allows the partitioning of the variance of a response matrix to explanatory matrices. We divided explanatory datasets into four groups: temperature-related including MAT and MAR, water-related including MAP and  $ET_p$ , simulation periods (history, 2030s and 2060s) and climate projection models (GCMs  $\times$  SSP). The result of VPA represents the percentage of explained variance by explanatory matrices and their intersections.

### Reporting summary

Further information on research design is available in the Nature Portfolio Reporting Summary linked to this article.

### Data availability

Daily historical climate data are available at <https://data.cma.cn/>. The soil database is freely available at [http://poles.tpdc.ac.cn/zh-hans/data/8ba0a731-5b0b-4e2f-8b95-8b29cc3c0f3a/?tdsourcetag=s\\_pctim\\_aiomsg](http://poles.tpdc.ac.cn/zh-hans/data/8ba0a731-5b0b-4e2f-8b95-8b29cc3c0f3a/?tdsourcetag=s_pctim_aiomsg). The raw datasets from CMIP6 simulations are available at <https://esgf-node.lnl.gov/projects/cmip6/>. The bias correction method is available at <https://www.isimip.org/gettingstarted/isimip3b-bias-adjustment/>. The APSIM Classic is freely available at <https://www.apsim.info/download-apsim/>. The data needed to regenerate

the results in this study are publicly available at [https://figshare.com/articles/figure/\\_b\\_Data\\_for\\_Spatiotemporal\\_co-optimization\\_of\\_agricultural\\_management\\_practices\\_b\\_/24471919](https://figshare.com/articles/figure/_b_Data_for_Spatiotemporal_co-optimization_of_agricultural_management_practices_b_/24471919).

### Code availability

The code used to generate the results can be accessed at [https://figshare.com/articles/figure/\\_b\\_Data\\_for\\_Spatiotemporal\\_co-optimization\\_of\\_agricultural\\_management\\_practices\\_b\\_/24471919](https://figshare.com/articles/figure/_b_Data_for_Spatiotemporal_co-optimization_of_agricultural_management_practices_b_/24471919).

### References

- Shang, Z. et al. Can cropland management practices lower net greenhouse emissions without compromising yield? *Glob. Change Biol.* **27**, 4657–4670 (2021).
- Cui, Z. et al. Pursuing sustainable productivity with millions of smallholder farmers. *Nature* **555**, 363–366 (2018).
- Chen, X.-P. et al. Integrated soil–crop system management for food security. *Proc. Natl Acad. Sci. USA* **108**, 6399–6404 (2011).
- Du, Y. et al. A synthetic analysis of the effect of water and nitrogen inputs on wheat yield and water- and nitrogen-use efficiencies in China. *Field Crops Res.* <https://doi.org/10.1016/j.fcr.2021.108105> (2021).
- He, M. et al. Long-term appropriate N management can continuously enhance gross N mineralization rates and crop yields in a maize–wheat rotation system. *Biol. Fertil. Soils* **59**, 501–511 (2021).
- Yu, C. et al. Managing nitrogen to restore water quality in China. *Nature* **567**, 516–520 (2019).
- Wang, L. et al. Nitrogen management to reduce GHG emissions while maintaining high crop productivity in temperate summer rainfall climate. *Field Crops Res.* <https://doi.org/10.1016/j.fcr.2022.108761> (2023).
- Xin, Y. & Tao, F. Developing climate-smart agricultural systems in the North China Plain. *Agr. Ecosyst. Environ.* **291**, 106791 (2020).
- Song, Q. et al. Effect of straw retention on carbon footprint under different cropping sequences in Northeast China. *Environ. Sci. Pollut. Res. Int.* **28**, 54792–54801 (2021).
- Amelung, W. et al. Towards a global-scale soil climate mitigation strategy. *Nat. Commun.* **11**, 5427 (2020).
- Zhang, L. et al. Planning maize hybrids adaptation to future climate change by integrating crop modelling with machine learning. *Environ. Res. Lett.* <https://doi.org/10.1088/1748-9326/ac32fd> (2021).
- Wang, L. et al. Optimal straw management co-benefits crop yield and soil carbon sequestration of intensive farming systems. *Land Degrad. Dev.* **34**, 2322–2333 (2023).
- Liu, C., Lu, M., Cui, J., Li, B. & Fang, C. Effects of straw carbon input on carbon dynamics in agricultural soils: a meta-analysis. *Glob. Change Biol.* **20**, 1366–1381 (2014).
- Prestele, R. & Verburg, P. H. The overlooked spatial dimension of climate-smart agriculture. *Glob. Change Biol.* (2019).
- Keating, B. A. et al. An overview of APSIM, a model designed for farming systems simulation. *Eur. J. Agron.* **18**, 267–288 (2003).
- Carberry, P. S. et al. Scope for improved eco-efficiency varies among diverse cropping systems. *Proc. Natl Acad. Sci. USA* **110**, 8381–8386 (2013).
- Zhao, Y. et al. Economics- and policy-driven organic carbon input enhancement dominates soil organic carbon accumulation in Chinese croplands. *Proc. Natl Acad. Sci. USA* **115**, 4045–4050 (2018).
- Jägermeyr, J. et al. Climate impacts on global agriculture emerge earlier in new generation of climate and crop models. *Nat. Food* **2**, 873–885 (2021).

19. Liu, B. et al. Similar estimates of temperature impacts on global wheat yield by three independent methods. *Nat. Clim. Change* **11**, 1130–1136 (2016).
20. Kimball, B. A. Crop responses to elevated CO<sub>2</sub> and interactions with H<sub>2</sub>O, N, and temperature. *Curr. Opin. Plant Biol.* **31**, 36–43 (2016).
21. Lobell, D. B., Deines, J. M. & Tommaso, S. D. Changes in the drought sensitivity of US maize yields. *Nat. Food* <https://doi.org/10.1038/s43016-020-00165-w> (2020).
22. Wood, S. A. & Bowman, M. Large-scale farmer-led experiment demonstrates positive impact of cover crops on multiple soil health indicators. *Nat. Food* **2**, 97–103 (2021).
23. Yin, Y. et al. A steady-state N balance approach for sustainable smallholder farming. *Proc. Natl Acad. Sci. USA* **118**, e2106576118 (2021).
24. Berhane Hagos, M. et al. Effects of long-term straw return on soil organic carbon storage and sequestration rate in North China upland crops: a meta-analysis. *Glob. Change Biol.* (2020).
25. Qiao, L. et al. Soil quality both increases crop production and improves resilience to climate change. *Nat. Clim. Change* **12**, 574–580 (2022).
26. Folberth, C. et al. Uncertainty in soil data can outweigh climate impact signals in global crop yield simulations. *Nat. Commun.* **7**, 11872 (2016).
27. Wang, E. et al. The uncertainty of crop yield projections is reduced by improved temperature response functions. *Nat. Plants* **3**, 17102 (2017).
28. Xiong, W. et al. Increased ranking change in wheat breeding under climate change. *Nat. Plants* **7**, 1207–1212 (2021).
29. Zhao, Z., Wang, E., Kirkegaard, J. A. & Rebetzke, G. J. Novel wheat varieties facilitate deep sowing to beat the heat of changing climates. *Nat. Clim. Change* **12**, 291–296 (2022).
30. Cai, S. et al. Optimal nitrogen rate strategy for sustainable rice production in China. *Nature* **615**, 73–79 (2023).
31. Xiao, L., Wang, G., Zhou, H., Jin, X. & Luo, Z. Coupling agricultural system models with machine learning to facilitate regional predictions of management practices and crop production. *Environ. Res. Lett.* **17**, 114027 (2022).
32. Zhang, X.-Q. et al. Tillage effects on carbon footprint and ecosystem services of climate regulation in a winter wheat–summer maize cropping system of the North China Plain. *Ecol. Indic.* **67**, 821–829 (2016).
33. Luo, N. et al. China can be self-sufficient in maize production by 2030 with optimal crop management. *Nat. Commun.* **14**, 2637 (2023).
34. *China Statistical Yearbook 2018* (National Bureau of Statistics of China, 2018).
35. Zhao, Z., Qin, X., Wang, Z. & Wang, E. Performance of different cropping systems across precipitation gradient in North China Plain. *Agric. For. Meteorol.* **259**, 162–172 (2018).
36. Ni, B. et al. Exponential relationship between N<sub>2</sub>O emission and fertilizer nitrogen input and mechanisms for improving fertilizer nitrogen efficiency under intensive plastic-shed vegetable production in China: a systematic analysis. *Agr. Ecosyst. Environ.* **312**, 107353 (2021).
37. *R: A Language and Environment for Statistical Computing*, version 4.0.5 (R Foundation for Statistical Computing, 2021).
38. Arias, P. et al. *Climate Change 2021: The Physical Science Basis. Contribution of Working Group I to the Sixth Assessment Report of the Intergovernmental Panel on Climate Change; Technical Summary* (IPCC, 2021).
39. O'Neill, B. C. et al. The Scenario Model Intercomparison Project (ScenarioMIP) for CMIP6. *Geosci. Model Dev.* **9**, 3461–3482 (2016).
40. Lange, S. Trend-preserving bias adjustment and statistical downscaling with ISIMIP3BASD (v1.0). *Geosci. Model Dev.* **12**, 3055–3070 (2019).
41. Wei, S. & Dai, Y. Dataset of soil properties for land surface modeling over China. *A Big Earth Data Platform for Three Poles* <https://doi.org/10.11888/Soil.tpd.270281> (2019).
42. Xu, M. G., Zhang, W. J. & Shuang, S. W. *China Soil Fertility Evolution* (2nd edition) 1124 (China Agriculture and Science Technology Publishing House, 2015).
43. Probert, M. E., Dimes, J. P., Keating, B. A., Dalal, R. C. & Strong, W. M. APSIM's water and nitrogen modules and simulation of the dynamics of water and nitrogen in fallow systems. *Agr. Syst.* **56**, 1–28 (1998).
44. Luo, Z. et al. Modelling soil carbon and nitrogen dynamics using measurable and conceptual soil organic matter pools in APSIM. *Agr. Ecosyst. Environ.* **186**, 94–104 (2014).
45. Thorburn, P. J., Biggs, J. S., Collins, K. & Probert, M. E. Using the APSIM model to estimate nitrous oxide emissions from diverse Australian sugarcane production systems. *Agr. Ecosyst. Environ.* **136**, 343–350 (2010).
46. Smith, C. et al. Measurements and APSIM modelling of soil C and N dynamics. *Soil Res.* **58**, 41–61 (2019).
47. Wang, G., Luo, Z., Wang, E. & Zhang, W. Reducing greenhouse gas emissions while maintaining yield in the croplands of Huang-Huai-Hai Plain, China. *Agr. For. Meteorol.* **260–261**, 80–94 (2018).
48. Liu, Z. et al. Optimization of China's maize and soy production can ensure feed sufficiency at lower nitrogen and carbon footprints. *Nat. Food* **2**, 426–433 (2021).
49. Reddy, S., et al. (2019). The 2019 Refinement to the 2006 IPCC guidelines for national greenhouse gas inventories (eds E. Calvo Buendia, K. Tanabe, A. Kranjc, J. Baasansuren, M. Fukuda, S. Ngarize, A. Osako, Y. Pyrozhenko, P. Shermanau, & S. Federici) (IPCC, 2019).
50. 2006 IPCC guidelines for national greenhouse gas inventories. *Institute for Global Environmental Strategies* (IPCC, 2006).
51. Mullen, K., Ardia, D., Gil, D. L., Windover, D. & Cline, J. DEoptim: an R package for global optimization by differential evolution. *J. Stat. Softw.* **40**, 1–26 (2011).
52. Tsou, C.-S. *nsga2R: Elitist Non-dominated Sorting Genetic Algorithm Based on R. R Package Version 1.0*. (R Foundation for Statistical Computing, 2013).
53. Peres-Neto, P. R., Legendre, P., Dray, S. & Borcard, D. Variation partitioning of species data matrices: estimation and comparison of fractions. *Ecology* **87**, 2614–2625 (2006).

## Acknowledgements

We acknowledge financial support from the national key research programme of Ministry of Science and Technology of China (grant no. 2021YFE0114500 to Z.L.) and the National Natural Science Foundation of China (grant no. 42001105 to L.X.) and the Fundamental Research Funds for the Central Universities (XUEKEN2023012, KYLH2023005 to L.X.).

## Author contributions

Z.L. conceived the study; L.X., G.W., P.Z. and H.Z. compiled the data; L.X., G.W. and H.Z. led the data assessment with the contributions of S.L.; L.X. conducted mapping; Z.L., L.X., G.W., E.W. and J.C. interpreted the results with the contribution of all authors; Z.L. and L.X. led manuscript writing with substantial contributions of all authors; Z.L., L.X. and Y.Z. contributed to the manuscript revision.

## Competing interests

The authors declare no competing interests.

## Additional information

**Supplementary information** The online version contains supplementary material available at <https://doi.org/10.1038/s43016-023-00891-x>.

**Correspondence and requests for materials** should be addressed to Zhongkui Luo.

**Peer review information** *Nature Food* thanks Fanqiao Meng, Jordi Sardans and Zhenling Cui for their contribution to the peer review of this work.

**Reprints and permissions information** is available at [www.nature.com/reprints](http://www.nature.com/reprints).

**Publisher's note** Springer Nature remains neutral with regard to jurisdictional claims in published maps and institutional affiliations.

Springer Nature or its licensor (e.g. a society or other partner) holds exclusive rights to this article under a publishing agreement with the author(s) or other rightsholder(s); author self-archiving of the accepted manuscript version of this article is solely governed by the terms of such publishing agreement and applicable law.

© The Author(s), under exclusive licence to Springer Nature Limited 2024



## Reporting Summary

Nature Portfolio wishes to improve the reproducibility of the work that we publish. This form provides structure for consistency and transparency in reporting. For further information on Nature Portfolio policies, see our [Editorial Policies](#) and the [Editorial Policy Checklist](#).

### Statistics

For all statistical analyses, confirm that the following items are present in the figure legend, table legend, main text, or Methods section.

n/a Confirmed

- |                                     |                                     |  |
|-------------------------------------|-------------------------------------|--|
| <input type="checkbox"/>            | <input checked="" type="checkbox"/> | The exact sample size ( $n$ ) for each experimental group/condition, given as a discrete number and unit of measurement  |
| <input checked="" type="checkbox"/> | <input type="checkbox"/>            | A statement on whether measurements were taken from distinct samples or whether the same sample was measured repeatedly  |
| <input type="checkbox"/>            | <input checked="" type="checkbox"/> | The statistical test(s) used AND whether they are one- or two-sided<br><i>Only common tests should be described solely by name; describe more complex techniques in the Methods section.</i>   |
| <input type="checkbox"/>            | <input checked="" type="checkbox"/> | A description of all covariates tested   |
| <input checked="" type="checkbox"/> | <input type="checkbox"/>            | A description of any assumptions or corrections, such as tests of normality and adjustment for multiple comparisons  |
| <input type="checkbox"/>            | <input checked="" type="checkbox"/> | A full description of the statistical parameters including central tendency (e.g. means) or other basic estimates (e.g. regression coefficient) AND variation (e.g. standard deviation) or associated estimates of uncertainty (e.g. confidence intervals) |
| <input type="checkbox"/>            | <input checked="" type="checkbox"/> | For null hypothesis testing, the test statistic (e.g. $F$ , $t$ , $r$ ) with confidence intervals, effect sizes, degrees of freedom and $P$ value noted<br><i>Give <math>P</math> values as exact values whenever suitable.</i>                            |
| <input checked="" type="checkbox"/> | <input type="checkbox"/>            | For Bayesian analysis, information on the choice of priors and Markov chain Monte Carlo settings   |
| <input type="checkbox"/>            | <input checked="" type="checkbox"/> | For hierarchical and complex designs, identification of the appropriate level for tests and full reporting of outcomes   |
| <input checked="" type="checkbox"/> | <input type="checkbox"/>            | Estimates of effect sizes (e.g. Cohen's $d$ , Pearson's $r$ ), indicating how they were calculated   |

Our web collection on [statistics for biologists](#) contains articles on many of the points above.

### Software and code

Policy information about [availability of computer code](#)

Data collection WebPlotDigitizer-4.2 software was used for data collection in published data.

Data analysis Computations, predictions and data visualization were performed using R 4.1.2.

For manuscripts utilizing custom algorithms or software that are central to the research but not yet described in published literature, software must be made available to editors and reviewers. We strongly encourage code deposition in a community repository (e.g. GitHub). See the Nature Portfolio [guidelines for submitting code & software](#) for further information.

### Data

Policy information about [availability of data](#)

All manuscripts must include a [data availability statement](#). This statement should provide the following information, where applicable:

- Accession codes, unique identifiers, or web links for publicly available datasets
- A description of any restrictions on data availability
- For clinical datasets or third party data, please ensure that the statement adheres to our [policy](#)

Daily historical climate data is available at <https://data.cma.cn/>. The soil database is freely available on at [http://poles.tpd.ac.cn/zh-hans/data/8ba0a731-5b0b-4e2f-8b95-8b29cc3c0f3a/?tdsourcetag=s\\_pctim\\_aiomsg](http://poles.tpd.ac.cn/zh-hans/data/8ba0a731-5b0b-4e2f-8b95-8b29cc3c0f3a/?tdsourcetag=s_pctim_aiomsg). The raw datasets from CMIP6 simulations are available at <https://esgf-node.llnl.gov/projects/cmip6/>. The bias correction method is available at <https://www.isimip.org/gettingstarted/isimip3b-bias-adjustment/>. The APSIM Classic is freely available at

<https://www.apsim.info/download-apsim/>. The data needed to evaluate the conclusions of this study are publicly available at: [https://figshare.com/articles/figure/\\_b\\_Data\\_for\\_Spatiotemporal\\_co-optimization\\_of\\_agricultural\\_management\\_practices\\_b\\_/24471919](https://figshare.com/articles/figure/_b_Data_for_Spatiotemporal_co-optimization_of_agricultural_management_practices_b_/24471919).

## Human research participants

Policy information about [studies involving human research participants and Sex and Gender in Research](#).

Reporting on sex and gender

Population characteristics

Recruitment

Ethics oversight

Note that full information on the approval of the study protocol must also be provided in the manuscript.

## Field-specific reporting

Please select the one below that is the best fit for your research. If you are not sure, read the appropriate sections before making your selection.

☐ Life sciences ☐ Behavioural & social sciences ☒ Ecological, evolutionary & environmental sciences

For a reference copy of the document with all sections, see [nature.com/documents/nr-reporting-summary-flat.pdf](https://www.nature.com/documents/nr-reporting-summary-flat.pdf)

## Ecological, evolutionary & environmental sciences study design

All studies must disclose on these points even when the disclosure is negative.

Study description	We develop a hybrid approach combining agricultural system modelling, machine learning, and life cycle assessment to enable spatiotemporally co-optimization of fertilizer application, irrigation and residue management, and apply the approach to predict optimal management to achieve yield potential and minimizing greenhouse gas emissions in the North China Plain - a key region of global wheat and maize production.
Research sample	In this study, we used historical meteorological data and soil data to run APSIM model. Nine long-term agricultural trials conducted in the North China Plain (NCP) were used to verify APSIM parameters. The farmers' actual practice and field experiment-based recommendation of management practices collected in published data were used to compare with our optimized management.
Sampling strategy	For the observational experiment-based data, we conducted a literature search to collect data about yield and relevant application of N fertilizers, irrigation amount and residue retention. A total of 307 observations including 108 values of N fertilizer use from 33 studies, 182 values of irrigation water use from 38 studies, and 17 values of residue retention fraction from seven studies were obtained. The observational practices can be divided into two general types: farmers' actual practice and field experiment-based recommendation of management practices. We calculated the N productivity and irrigation productivity (Fig. S11) as the ratio of yield to corresponding N input and irrigation amount. All data have been grouped into two types (i.e., farmers' practice and trial-based recommendation), and compared to model predictions in the similar period at the regional level. In addition, we extracted data from 12 long-term agricultural trials from 11 studies on long-term SOC changes, and 17 from 6 studies on N <sub>2</sub> O and GHG emission) with current farmer's conventional and recommended management practices for winter wheat-summer maize system during 1980-2017 in the region studied. For model simulation, 6000 grid-scenario simulation outputs from the APSIM model were selected to train machine learning models.
Data collection	Daily historical meteorological data at ~2400 climate stations across China (including 318 stations in NCP), including maximum temperature, minimum temperature, precipitation, sunshine hours, relative humidity and wind speed, were obtained for the period 1981-2014 from the Chinese Meteorological Administration ( <a href="http://data.cma.cn">http://data.cma.cn</a> ). We collected climate during the period from 2015 to 2070 for six general circulation models (GCMs, including BCC_CSM2_MR, HadGEM3_GC31_LL, FGOALS-g3, IPSL_CM6A_LR, GFDL_ESM4, MIROC6, Table S1) participating the Coupled Model Inter-comparison Project phase 6 (CMIP6), under two shared socio-economic pathways (i.e., SSP2-4.5 and SSP5-8.5). Soil data were obtained from the China Soil Scientific Database, which was generated based on more than 7000 soil profile measurements in the late 1970s/early 1980s across China and is the most comprehensive soil data available. We conducted a literature search to collect data about yield and relevant application of N fertilizers, irrigation amount and residue retention from published data. We collected data from nine long-term agricultural trials conducted in the North China Plain (NCP) as a part of the National Long-term Fertilization Experimental Network in China.
Timing and spatial scale	The spatial scale is ~1 km (1/120 degree) spatial resolution across the North China Plain (NCP) croplands. The model simulation data were simulated from 1981 to 2070. Three periods, 1995–2014 (as the historical reference period), 2030s: 2021–2040 (represents near future), and 2060s: 2051–2070 (represents distant future) were selected to optimized cropland management practices.
Data exclusions	None.
Reproducibility	Our study is an integrated study mainly based on model simulation ,statistical data and reference data. Our results can be

Reproducibility

reproduced when following the described methods and data.

Randomization

To solve this computational challenge, 6000 grid-scenarios were randomly drawn to run the APSIM model.

Blinding

No blinding was required.

Did the study involve field work?

☐

Yes

☒

No

## Reporting for specific materials, systems and methods

We require information from authors about some types of materials, experimental systems and methods used in many studies. Here, indicate whether each material, system or method listed is relevant to your study. If you are not sure if a list item applies to your research, read the appropriate section before selecting a response.

### Materials & experimental systems

n/a	Involved in the study
<input checked="" type="checkbox"/>	<input type="checkbox"/> Antibodies
<input checked="" type="checkbox"/>	<input type="checkbox"/> Eukaryotic cell lines
<input checked="" type="checkbox"/>	<input type="checkbox"/> Palaeontology and archaeology
<input checked="" type="checkbox"/>	<input type="checkbox"/> Animals and other organisms
<input checked="" type="checkbox"/>	<input type="checkbox"/> Clinical data
<input checked="" type="checkbox"/>	<input type="checkbox"/> Dual use research of concern

### Methods

n/a	Involved in the study
<input checked="" type="checkbox"/>	<input type="checkbox"/> ChIP-seq
<input checked="" type="checkbox"/>	<input type="checkbox"/> Flow cytometry
<input checked="" type="checkbox"/>	<input type="checkbox"/> MRI-based neuroimaging